Astron. Astrophys. 330, 975–989 (1998)

ASTRONOMY
AND
ASTROPHYSICS

Kinematic signatures of violent formation of galactic OB associations from Hipparcos measurements

F. Comerón[1], **J. Torra**[2], **and A.E. Gómez**[3]

[1] European Southern Observatory, Karl-Schwarzschild-Strasse 2, D-85748 Garching bei München, Germany (fcomeron@eso.org)
[2] Departament d'Astronomia i Meteorologia, Universitat de Barcelona, Av. Diagonal, 647, E-08028 Barcelona, Spain (jordi@mizar.am.ub.es)
[3] Département d'Astrophysique Stellaire et Galactique, Observatoire de Paris-Meudon, F-92195 Meudon, France (anita@mehipa.obspm.fr)

Received 23 May 1997 / Accepted 27 October 1997

Abstract. Proper motions measured by *Hipparcos* confirm the large anomalous velocities of the OB associations located around the Cygnus Superbubble (Cygnus OB1, OB3, OB7, and OB9), and reveal a clearly organized expanding pattern in Canis Major OB1. At the distances of these associations, the organized velocity patterns imply LSR velocities of up to $\sim$ 60 km s^{-1} for the associations in Cygnus, and about $\sim$ 15 km s^{-1} in Canis Major OB1. The magnitude and spatial arrangement of the expanding motions suggests that very energetic phenomena are responsible for the formation of the present OB associations. This is independently supported by observations of the associated interstellar medium carried out in other wavelengths.

The gravitational instability scenario proposed by Comerón & Torra 1994 (ApJ 423, 652) to account for the formation of the stars in the Cygnus Superbubble region is reviewed in the light of the new kinematic data. It is found that the energetic requirements set by the highest velocities on the OB association powering the Superbubble, Cygnus OB2, are too large by orders of magnitude. However, the scenario can still account for the formation of most of the stars if, as can be reasonably expected, the stars with the highest measured velocities are actually runaways from Cygnus OB2 itself.

As for Canis Major OB1, we consider their formation in a supernova remnant, as suggested by Herbst & Assousa 1977 (ApJ, 217, 473). The detection of a new runaway star, HIC 35707 (=HD 57682), whose motion is directed away from the derived center of expansion, supports this scenario and provides an independent age for the supernova remnant, assuming that the runaway star was the binary companion of the supernova. Based on a number of arguments, however, we find it unlikely that the stars are a direct consequence of instabilities in the expanding shell. We propose instead that their formation was triggered in preexisting clouds, accelerated and compressed by the supernova explosion.

Key words: stars: early type; formation; kinematics – ISM: bubbles – Galaxy: open cluster and associations

1. Introduction

The unprecedented accuracy of the proper motions and parallaxes obtained by the astrometric satellite *Hipparcos* is opening a new era in the calibration of fundamental stellar properties, as well as in kinematic studies of the solar neighbourhood. Even for stars several hundred parsecs away from the Sun, too distant for their trigonometric parallaxes to be measured by *Hipparcos*, the quality of *Hipparcos* proper motions allows to determine velocities in the plane of the sky with a precission of a few km s^{-1} when combined with photometry and spectroscopy. Such a wealth of data makes it possible to study in detail deviations from the circular galactic rotation.

An interesting kind of deviations from the standard galactic rotation may be caused by energetic processes taking place in the galactic disk, such as those associated to photoionization and stellar winds from massive stars, supernova explosions, or high velocity cloud impacts on the galactic disk (Elmegreen & Lada 1977, McCray & Kafatos 1987, Tenorio-Tagle & Palous 1987, Palous et al. 1990, 1994, Comerón & Torra 1992, 1994b, Whitworth et al. 1994, Elmegreen et al. 1995). All these processes can compress and accelerate the interstellar gas triggering star formation, and it is conceivable that the motions of the stars formed in this way may preserve a record of such accelerations. Propagating star formation triggered by OB associations or supernovae has been invoked to explain structures seen in the Large Magellanic Cloud (Vallenari et al. 1993, Domgoergen et al. 1995, Oey & Massey 1995, Will et al. 1996, Rosado et al. 1996) or in M33 (Palous 1991, Oey & Massey 1994). However, the observation of the expected consequences of this mode of star formation on the kinematics of the stars are obviously elusive. Evidence for anomalous velocities in the Cygnus Superbubble region was found by Comerón et al. 1993 (hereafter CTGJ93)

Send offprint requests to: F. Comerón

using ground-based proper motion measurements. The expanding pattern was then interpreted by Comerón & Torra 1994a (hereafter CT94) in terms of gravitational instabilities in an expanding shell produced by the energetic activity of Cygnus OB2, a very rich and compact association lying at the center of the Cygnus Superbubble.

We have reanalyzed the kinematic data presented in CTGJ93 in order to confirm the reality of the anomaly, and to better characterize the expanding pattern thanks to the better quality of the *Hipparcos* data. At the same time, we have looked for structures similar to that seen in Cygnus in other regions of the galactic disk. Our results reveal that the stars forming the Canis Major OB1 association also move with a recognizeable expanding pattern, in agreement with the hypothesis of Herbst & Assousa 1977, who suggested that the formation of this association was triggered by a supernova event. The interpretation of both the Cygnus and Canis Major regions in the framework of violent star formation processes is discussed in the present paper.

2. Observational data

The observational database of this study consists of the stars selected for measurements by *Hipparcos* for the proposal *Young stars: irregularities of the velocity field and spiral structure*. The global sample consists of 6290 stars with spectral types O and B contained in the Hipparcos Input Catalogue (Turon et al. 1992). The completeness in magnitude of the sample is mainly a function of the spectral type, and to a lesser extent also of the galactic latitude.

Our main interest in the present paper lies in studying irregularities in the motions of groups of young stars beyond the local system, dominated by the Gould Belt (Comerón & Torra 1994b, Comerón et al. 1994, Pöppel 1997). This places our objects of interest at distances greater than $\sim$ 500 pc. At these distances, the trigonometric parallaxes measured by Hipparcos are uncertain by about 50 %, and they are well under their errors at the estimated distance of the associations in Cygnus. On the other hand, given the relatively large uncertainties subsisting in photometric parallaxes calculated from UBV photometry and spectral types (see e.g. de Geus 1990, Luri 1995), we have tried to make our selection of objects and our analysis as independent as possible of the individual stellar distances.

To carry out our study, we defined a subsample of "distant" stars, excluding those for which the parallax measured by *Hipparcos* exceeds 0"003. We then retained in the sample only spectral types B2 or earlier for luminosity classes IV-V, B4 or earlier for luminosity classes II-III, and all O and B types for luminosity class I. BV photometry and spectral types are those compiled in the Hipparcos Input Catalogue (Turon et al. 1992). Stars lying 5^0 or more from the galactic plane were also excluded. The sample defined in this way contains 1092 stars, whose proper motions are typically accurate to within 0.8 mas yr^{-1}, corresponding to a velocity in the plane of the sky of 3 km s^{-1} at a distance of 1 kpc[1].

3. Analysis

3.1. Overview of motions parallel to the galactic plane

Fig. 1 shows the distribution of all the stars in our sample in a $l - \mu_l \cos b$ diagram, where (l, b) are galactic longitude and latitude, and (μ_l, μ_b) are proper motions in l and b. Superimposed in the diagram are curves showing the expected μ_l for stars at $b = 0^0$ located at different distances from the Sun, calculated according to

$$\mu_l = \frac{1}{r}(1.56 \sin l - 3.22 \cos l) + 2.74 \cos 2l - 2.74 \quad (1)$$

where μ_l is in mas yr^{-1} and r is in kiloparsecs. This formula results from the first-order development applicable to stars at distances r small as compared with the distance to the galactic center (e.g. Scheffler & Elsässer 1987). For the coefficients in this formula, a flat rotation curve was assumed with Oort constants $A = -B = 13$ km s^{-1} kpc^{-1}. The components of the solar motion towards the galactic center and in the direction of galactic rotation were taken as $(U_\odot, V_\odot) = (7.4, 15.3)$ km s^{-1} (Comerón et al. 1994, for O - B5.5 stars within 1500 pc from the Sun).

The most evident feature in Fig. 1 is the double-sine shape followed by distant stars reflecting galactic rotation, while nearby stars are dominated by their peculiar motion and the reflection of the solar peculiar velocity. As could be expected from our selection criteria, most of the stars lie in the region of $r > 1$ kpc. Clusters of points at different galactic longitudes represent known associations (Humphreys et al. 1978, Garmany & Stencel 1992) and groups of associations which trace spiral arms (Schmidt-Kaler 1975, Elmegreen 1985). The group at $10^0 < l < 20^0$ is formed by the most luminous stars in the distant OB associations of Sagittarius, Serpens and Scutum, belonging to the Sagittarius arm. The conspicuous cluster of points at $70^0 < l < 80^0$, centered at $\mu_l = -7.5$ mas yr^{-1}, corresponds to the group of associations in the western part of the Cygnus Superbubble reported by CTGJ93, that we will discuss in detail in the next Sections. Note that this group falls in a region of the $l - \mu_l$ diagram forbidden by galactic rotation, regardless of the adopted distance. The group centered at $(l, \mu_l) \simeq (135, 0)$ is the Perseus OB1 association. The band of points between $280^0 < l < 310^0$ corresponds to the OB associations in Carina, Centaurus and Crux which delineate the Carina-Centaurus spiral arm. An intriguing feature of this region is the migration of points from above the $r = 1$ kpc curve at $l = 280^0$ to the proximities of the curve expected for stars lying at larger distances from the Sun, around $l = 310^0$. The Carina- Centaurus arm,

[1] For notation convenience, we will express proper motions in mas yr^{-1}, rather than the more commonly used arcsec yr^{-1}; 1 mas yr^{-1} = 0"001 yr^{-1}.

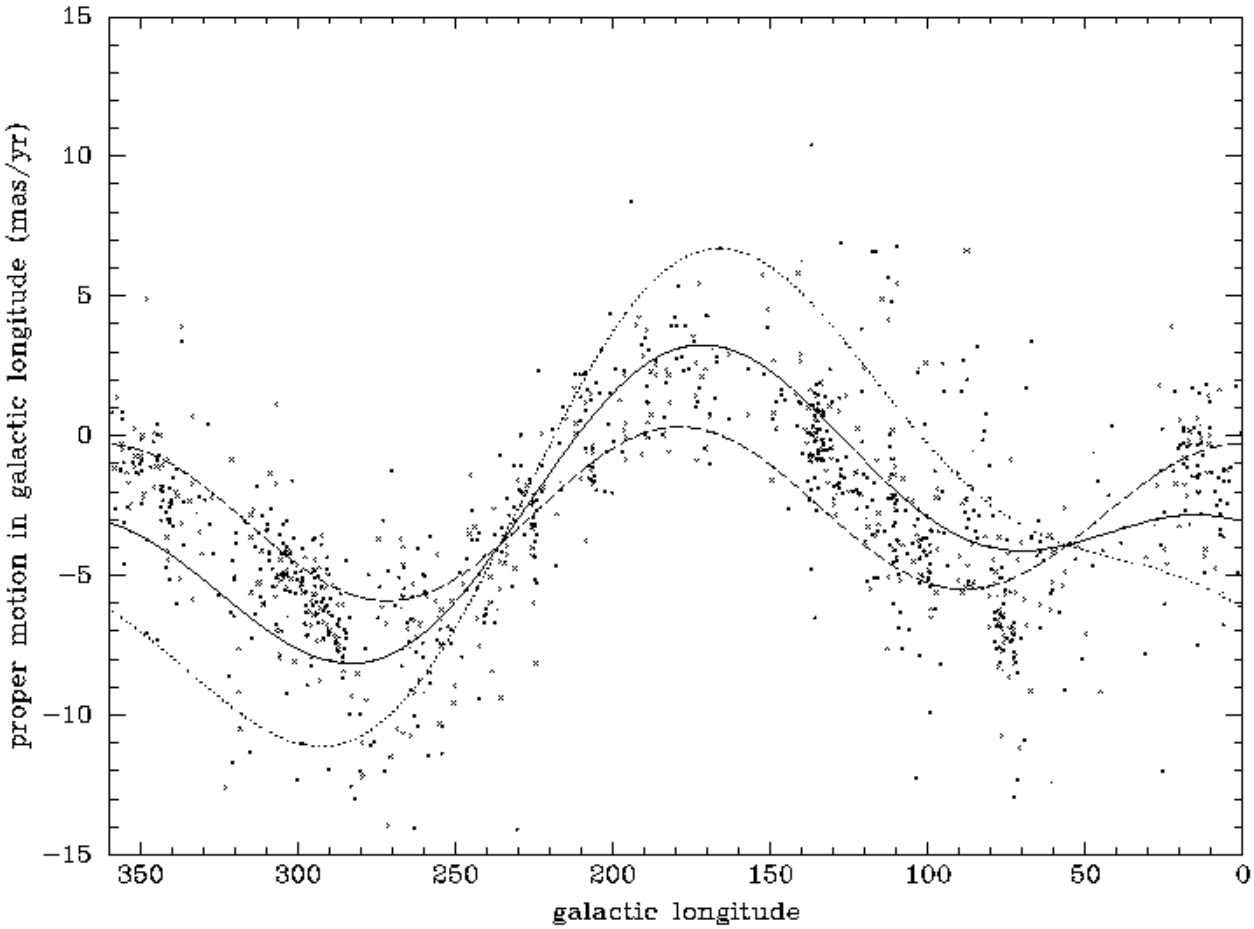

Fig. 1. Distribution of stars in galactic longitude vs. proper motion in galactic longitude. The lines represent the systematic proper motions expected from the circular galactic rotation and the solar peculiar velocity for stars located at different distances from the Sun: r = 0.5 kpc (dotted line), r = 1 kpc (solid line) and $r = \infty$ (dashed line). The latter represents the motions of distant stars for which the reflection of the solar motion (decreasing as $1/r$) is insignificant as compared to the galactic rotation (independent of r). It is assumed that all the stars are nearby enough so that the first order approximation to the galactic rotation curve leading to Eq. (1) is valid.

whose connection with the Sagittarius arm seems well established, has been extensively mapped in several tracers (Vogt & Moffat 1975; Humphreys 1976; Grabelsky et al. 1988; Alvarez et al. 1990). All the derived maps coincide in placing the arm at *decreasing* distances from the Sun as the galactic longitude increases, contrarily to the trend seen in Fig. 1. Interestingly, the points closer to the dashed curve cluster around $l = 305^0$; Humphreys 1976 has suggested the existence of a "spur" in the Carina-Centaurus arm at this location, where young objects can be traced with distances between 2 and 5 kpc from the Sun. The points located near the $r = \infty$ curve may thus correspond to stars belonging to this spur. An alternative explanation could be based on streaming motions associated to spiral arms; if so, the streaming velocity required to reproduce the observed position of these points would exceed 20 km s^{-1} if the stars are located at $r \simeq 2$ kpc. This feature was already predicted at this position by Lin et al. 1978, who studied the kinematics that nearby stars should display in the presence of the non-linear effects induced by spiral density waves on the motion of the gas from which they formed. Although the amplitude of streaming motions appearing in the rotation curve of our Galaxy seem to be much smaller (Clemens 1985), global spiral shocks have been proposed by Comerón et al. 1997 as a way to explain the origin of moving groups in the solar neighbourhood, whose deviations from the circular rotation are also of order 20 km s^{-1}; such a mechanism may also have been at work in the Carina arm. In any case, a closer inspection at this region shows that the pattern of motions is not suggestive of an expanding structure such as those discussed in the present paper, and we will not discuss it further, although it certainly deserves a future detailed investigation.

3.2. Expanding patterns

A closer inspection at the data was carried out by plotting the peculiar motions of stars in different region of the galactic disk, after having subtracted the systematic motion given by Eq. (1) for r = 1 kpc. For more distant regions concentrated in a narrow range of galactic longitudes, a distance very different from the

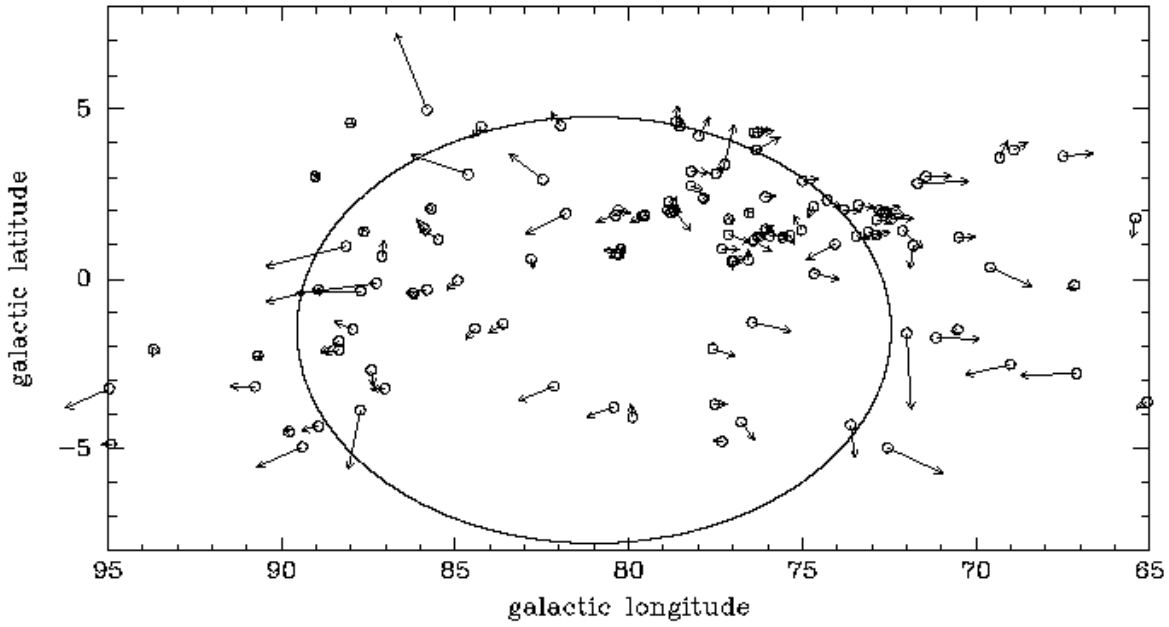

Fig. 2. Positions and velocities of stars in the Cygnus region. The arrows represent residual motions in the plane of the sky, after subtraction of systematic motions according to Eq. (1). The largest residual motion represented corresponds to the star at l = 85^{0}81, b = 4^{0}98, and is 9.8 mas yr^{-1}. A distance of 1.25 kpc has been assumed to subtract the expected systematic motion. The ellipse represents the approximate outer limits of the Cygnus Superbubble, as given by Cash et al. 1980.

adopted one should result in a constant shift of the proper motions, although this shift would not exceed $\sim$ 2 mas yr^{-1} in the most unfavourable case. The plots were then visually examined to search for any obvious expanding structures which may be present. At young ages, such expanding structures should reveal themselves simply as arrangements of stars seemingly radiating away from a small region of the celestial sphere. When the age of the expanding structure becomes a significant fraction of the epicyclic period $2\pi/\kappa$ ($\simeq 1.7 \times 10^8$ yr in the solar neighbourhood), the initially radial expanding motions become distorted by the differential rotation of the galactic disk, and the expansion becomes more difficult to recognize (e.g. Lindblad et al. 1973, Olano & Pöppel 1987). However, given the spectral types of the stars considered here and the young age of OB associations, we can expect to deal with structures younger than $\sim 10^7$ yr, for which the radial expansion approximation should still be valid.

We could clearly identify two expanding structures in our plots. The first of them, shown in Fig. 2, corresponds to the Cygnus region, whose western part (l between 70^0 and 80^0) makes up the clump of points with forbidden positions discussed in Sect. 3.1, and identified with the associations Cygnus OB1, OB3, and OB9. This is the region discussed in detail by CTGJ93. The actual systematic proper motion subtracted in Fig. 2 from the measured components is that corresponding to a more likely distance of 1.25 kpc, as discussed in Sect. 4.1. Interestingly, the stars in the eastern part of the region tend to have motions in the opposite direction, completing the expanding ring. Hints of this behaviour can already be seen in Fig. 2 of CTGJ93 but, due to the scarcity of points in that region and the inferior quality of pre-*Hipparcos data*, this feature was not discussed by those authors.

The other expanding structure identified in our data comprises a set of about 20 stars in the area $224^0 < l < 230^0$, $-4^0 < b < +3^0$, which seem to delineate a hemispherical shell (Fig. 3). The southern part of this region coincides with the Canis Major OB1 - R1 complex. The extension to the North is suggested by a single star, HIC 35707 (=HD 57682), whose high proper motion is indicative of a runaway and is directed away from the center of expansion. The systematic contribution subtracted to the proper motions to obtain the peculiar motions displayed in Fig. 3 is that corresponding to a distance of 1.15 kpc (see Sect. 4.2).

A rough determination of the expansion centers and the expansion age was carried out by defining the sum S of the squares of the projected distance of each star i to a point of coordinates (l_e, b_e) at a time t in the past:

$$S = \sum_i \left[(l_i - \mu_{li}^r t - l_e)^2 + (b_i - \mu_{bi}^r t - b_e)^2 \right] \qquad (2)$$

where μ_l^r, μ_b^r indicates residual proper motions after subtraction of the systematic component (1). The function S was then minimized with respect to l_e, b_e, and t, thus obtaining an estimate of the galactic longitude and latitude of the expansion center and the expansion age. As a first step, all the stars in the areas ($67^0 < l < 92^0$ for Cygnus, $233^0 < l < 230^0$ for Canis Major) were included in the sum of Eq. (2). The derivation was then refined by repeating the calculation, but now including in the sum only those stars for which

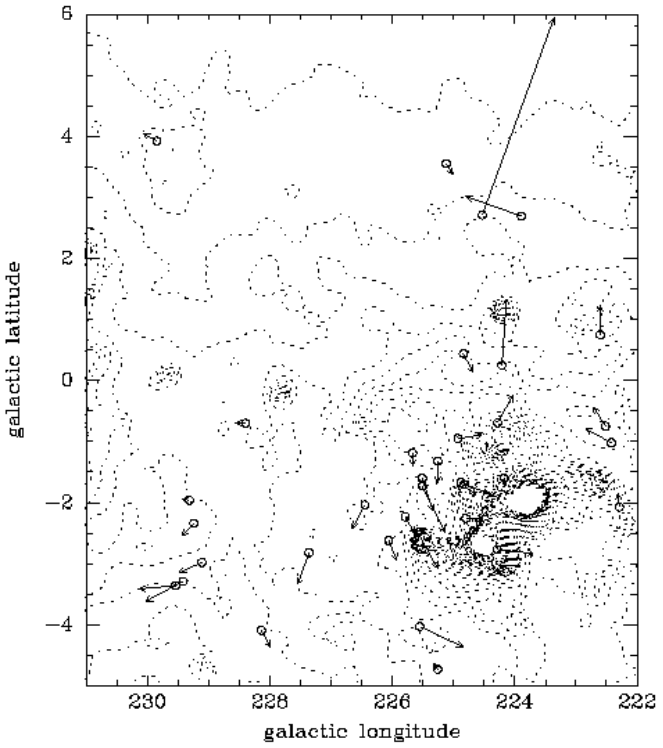

Fig. 3. Positions and velocities of stars in the Canis Major region. The arrows represent residual motions in the plane of the sky, after subtraction of systematic motions according to Eq. (1). A distance of 1.15 kpc has been assumed. The dashed lines represent intensity contours of the 100 μ emission detected by IRAS. The main concentration of emission in the southwest contains the HII regions S292, S293, S295, and S296.

Table 1. Expansion centers and ages

	l_e	b_e	t
Cygnus	$79^0 0$	$+0^0 9$	$3.6 \cdot 10^6$ yr
Canis Major	$226^0 5$	$-1^0 6$	$1.5 \cdot 10^6$ yr

$$(l_i - l_e)\mu^r_{li} + (b_i - b_e)\mu^r_{bi} > 0 \qquad (3)$$

The expansion centers and expansion ages found are given in Table 1.

The estimates presented in Table 1 are very probably contaminated by nonmembers which just happen to have their motion in a direction similar to that of the expansion, and are thus included in the calculation of S. Unrelated stars with small residual motions lying far from the expansion center will tend in general to increase the derived expansion age. Moreover, the expansion age is physically meaningful only as long as the stars are supposed to have formed together right at the expansion center, which may not be necessarily the case (Sect. 4.3). However, the positions of the expansion centers as given in Table 1 are close to what visual inspection of Figs. 2 and 3 suggests, and therefore we will adopt them as a reference. The expansion age, on the other hand, is of the order of the ages expected for the young stars discussed here and gives a characteristic timescale for the population.

3.3. Could a spiral shock produce the observed expanding patterns?

Before proceeding with our analysis, it is important to ensure that the expanding patterns that we identify in our data are truly indicative of a local phenomenon, rather than an illusory effect caused by streaming motions at larger scales. This seems fairly obvious in the case of Canis Major OB1 from Fig. 3, as the expanding pattern displays a fairly clear hemispherical geometry.

In the case of Cygnus, its location in a spiral arm and its greater spatial extent require a more careful assessment of other possibilities. Lin et al. 1978 showed that relatively large jumps in both proper motion and radial velocity may arise when the stars are formed in a global spiral shock. Such jumps may appear as group motions mimicking an expansion if viewed under the appropriate geometry. Moreover, a global expansion is expected in the interarm region, although its estimated rate (~ 5 km s^{-1} kpc^{-1} at most) makes it negligible over the sizes of the regions considered in the present paper.

Let us consider that the line of sight in the direction of Cygnus runs roughly parallel to a spiral arm (see Sect. 4.1). We will assume the spiral pattern to be trailing, with the solar neighbourhood inside the corotation circle. Under the influence of the density wave potential well, a parcel of gas approaching the spiral shock will initially increase its galactocentric distance (Roberts 1969, Lin et al. 1978) until crossing the shock front, at whose position the velocity component perpendicular to the shock is greatly reduced (Comerón et al. 1997). This causes the shocked gas to move with a radial component directed towards the galactic center. If a spiral shock exists at the position of Cygnus, therefore, objects following the path of the gas would initially have a peculiar proper motion in galactic longitude (i.e., a contribution superimposed on the overall double-sine pattern) with a positive sign, which could turn negative after crossing the shock. Whether this would result into an apparent expansion or contraction depends on the angle between the line of sight and the shock front: when this angle is small, as in the case of Cygnus, both streaming motions could be expected to overlap. To force agreement with the observed trends, we may assume that the Cygnus arm shock is tilted with respect to the line of sight, so that its galactic longitude grows as it gets closer to the Sun. In this way, the western part of the expanding pattern would correspond to distant stars formed out of shocked gas, while the eastern part would be composed of more nearby stars formed from gas still moving towards the shock. Although there are some indications that the eastern part is on the average somewhat closer to the Sun (Sect. 4.1), we believe that an interpretation of the observed pattern in Cygnus in terms of a spiral shock is rather unlikely, based on the following arguments:

a) The pattern of proper motions predicted by the shock hypothesis would not be reflected in the proper motions in galactic latitude, except for perspective effects due to group motions

Table 2. Candidate members of the Cygnus expanding structure

HIC	$l(^0)$	$b(^0)$	$\mu_l \cos b$ (mas yr^{-1})	μ_b (mas yr^{-1})	V	$(B-V)$	spectral type
97485	68.92	3.80	-6.79	0.25	6.42	0.13	B0.5Ibvar
98298	71.45	3.02	-8.49	-0.72	8.84	0.73	B0Ib
98982	76.30	4.32	-7.40	-0.62	9.50	0.04	B2
98999	72.67	1.96	-6.71	-1.33	7.29	0.20	B1Ib
99008	76.39	4.31	-7.13	-0.44	8.21	0.09	B0IVp
99061	72.11	1.42	-7.83	-3.49	8.59	0.31	B0III
99088	73.39	2.18	-7.33	-1.22	7.97	0.22	B0.5III
99122	72.86	1.74	-7.11	-1.24	7.26	0.09	B0III
99231	73.80	2.05	-7.38	-1.08	7.43	0.06	B0.5III
99283	72.87	1.30	-6.97	-0.40	7.38	0.13	B0.5IV
99437	73.45	1.26	-7.05	-1.16	7.79	0.08	B1III
99443	78.64	4.63	-5.29	1.62	8.28	0.31	O9.5IV
99469	78.52	4.49	-4.86	0.86	8.75	0.22	B0IV
99649	76.07	2.41	-6.53	-0.67	7.08	0.50	B0.5Ib
99760	77.49	3.10	-6.26	0.21	7.53	0.55	B0Ia
99898	75.36	1.28	-5.66	-2.23	10.20	0.35	B1V
99905	78.20	3.17	-7.60	-1.04	7.84	-0.03	B1Vn
99944	76.54	1.95	-4.73	-0.42	8.33	0.33	B0III
99980	75.56	1.22	-5.52	-1.13	7.64	0.26	B0.5II
100009	76.06	1.46	-6.03	-1.14	6.99	0.44	B1.5Ib
100124	77.85	2.38	-5.74	-0.48	7.73	1.01	B9Ia
100146	76.26	1.25	-7.17	0.78	7.26	0.33	O9III
100227	76.40	1.15	-6.41	0.05	8.68	0.46	B0Vp
100351	77.13	1.31	-8.13	-2.10	7.75	0.26	B2III
100409	81.96	4.51	-3.59	1.18	7.47	0.73	B1Ib
100484	76.56	0.56	-5.08	0.63	8.53	1.06	B1Iab
100548	78.79	1.95	-6.55	-0.65	7.03	0.86	B1.5Ia
100557	77.32	0.89	-7.54	-0.96	8.39	0.74	B0Ib
100600	76.98	0.54	-6.82	-0.51	9.36	0.67	B0II
100612	77.03	0.52	-5.09	-2.02	8.99	0.73	B0II
100771	79.55	1.88	-2.87	-1.98	7.77	0.23	B3II
100804	79.63	1.84	-4.45	-1.13	7.47	0.85	B0.5Ia
100987	80.38	1.88	-2.26	-1.81	7.66	0.12	B0.2III

along the line of sight. However, as Fig. 2 clearly shows, stars at positive galactic latitudes tend to have positive proper motions in galactic latitude, the opposite being true for those under the galactic equator. The perspective effects referred to could account for the magnitude of these trends only if the stars in the Cygnus region were moving toward the Sun at velocities of order of 100 km s^{-1}.

b) The spiral shock should account not only for the kinematical features of young stars, but for their very formation. Explaining the motions in the eastern side of Cygnus in terms of streaming motions induced by spiral arms would imply that the stars in this region are formed prior to the passage of their parental gas by the shock, precisely where the theory of the global spiral shock predicts the density to reach a minimum (Shu et al. 1972).

Moreover, the spatial coincidence of different structures probably related to very energetic events in the region under study, to be discussed in the next section, argues in favour of violent, local processes as the reason for the anomalous proper motions observed.

4. Discussion

4.1. The Cygnus region

The region where anomalous proper motions are detected has been widely studied in virtually all wavelengths (Cash et al. 1980, Wendker 1984, Bochkarev & Sitnik 1985, Piepenbrink & Wendker 1988, Odenwald 1989, Wendker et al 1991, Odenwald & Schwarz 1993, Dewdney & Lozinskaya 1994, and references in those works). The region is rich in tracers of recent star formation overlapping along the line of sight, which runs parallel to the axis of the local spiral arm. Cygnus X, an extended aggregate of molecular clouds, star forming and HII regions, lies in the southwestern part of the map shown in Fig. 2 (see Wendker et al. 1991 and references therein). The Cygnus Superbubble, a X-ray emitting region with dimensions $\sim 18^0 \times 13^0$ elongated along the galactic plane, was first detected by the HEAO-1 satellite (Cash et al. 1980). It approximately occupies the region over which the expanding motions are detected, as can be seen in Fig. 2, although only its northern part is observed, probably due to the heavier extinction in the South. Near its center is

Table 2. (continued)

HIC	$l(^0)$	$b(^0)$	$\mu_l \cos b$ (mas yr^{-1})	μ_b (mas yr^{-1})	V	$(B-V)$	spectral type
101186	82.47	2.93	-0.14	2.94	7.10	0.85	O9.5Ia
101350	85.81	4.98	-0.55	10.50	6.98	-0.08	B0V
101411	72.55	-4.96	-12.94	-4.65	7.79	0.03	B1.5V
101442	73.61	-4.29	-5.59	-5.63	7.34	-0.15	B2V
101648	77.58	-2.05	-8.27	-1.99	8.94	0.56	O9V
101729	84.63	3.08	3.19	2.05	9.39	0.75	B0III
102195	76.76	-4.21	-6.91	-3.51	6.70	-0.16	B2IV-V e
102722	85.49	1.16	-2.67	0.70	8.58	0.41	B1III
102724	85.87	1.47	-3.88	0.61	4.81	0.57	B3Ia
103061	83.62	-1.31	-2.87	-2.27	8.43	0.50	B0V
104361	88.93	-0.31	2.70	-2.70	7.91	-0.05	B0V
104454	87.94	-1.48	-2.28	0.27	7.66	-0.03	B2Vn...
104709	88.35	-1.83	-2.28	-2.54	8.63	-0.04	B2V
104742	87.02	-3.22	-2.99	-0.99	7.71	0.16	B2III
104787	88.34	-2.09	-2.73	-1.33	7.52	-0.11	B1V

Cygnus OB2, an association rich in O-type stars (Torres-Dodgen et al. 1991). The X-ray contours of the Superbubble are approximately traced by an ensemble of Hα filaments (Brand & Zealey 1975).

The evolution of the Cygnus Superbubble has been studied by Higdon 1981 and Abbott et al. 1981, but its real existence has been debated by Bochkarev & Sitnik 1985, who favour instead a casual arrangement of discrete X-ray sources along the line of sight. However, the coincidence of Cygnus OB2, the Superbubble, the Hα filaments, and the expanding motions of the stars around the Superbubble support a scenario relating all these features: the energetic activity of the massive stars in Cygnus OB2 would have produced a large sphere of hot gas (the Superbubble), surrounded by a dense shell of accumulated material, the inner part of which (the Hα filaments) is ionized by the stars of Cygnus OB2. Gravitational instabilities in the shell may then have produced the stars of the other OB associations, their motions reflecting the expansion of the shell (see Sect. 5). Other shells centered in the Cygnus OB1 - OB3 associations are seen in the infrared (Saken et al. 1992), the ultraviolet (Phillips et al. 1984, St.-Louis & Smith 1991), and HI (Dewdney & Lozinskaya 1994).

The distances to the structures observed in Cygnus are in general poorly determined. For extended sources, radial velocities are of limited help in deriving kinematic distances due to the small radial velocity gradient along the line of sight in this direction. As to the stellar component, although more accurate distances can be in principle computed from photometry and spectral types, the situation is also very confused. The distances to the associations in the area of the Cygnus Superbubble (Cygnus OB1, OB2, OB3, OB7, OB8, OB9) are made uncertain by factors such as the contamination by foreground and background stars (Massey et al. 1995), difficulties in calibrating the absolute magnitudes of the brightest stars (Torres-Dodgen et al. 1991), and uncertainties in the total-to-selective extinction ratio (Terranegra et al. 1994). Specific problems related to the determination of distances using Strömgren photometry were already discussed by CTGJ93. As a consequence, even the physical distinction among overlapping associations may not be real.

Summaries on these associations have been given by Humphreys 1978, Ruprecht 1981, and Garmany & Stencel 1992. New distance determinations appeared more recently have not settled the discrepancies (CTGJ93, Terranegra et al. 1994, Massey et al. 1995), with distances to different structures (and often to the same structure!) varying between less than 1 kpc to about 2.5 kpc. Although a part of these discrepancies can be due to a real spread in heliocentric distances, the contribution from observational and calibration uncertainties is important, if not dominant. We should point out, on the other hand, that if the extent of the whole structure in the radial direction is comparable to that in the plane of the sky, then one may expect to find a spread of distances exceeding 400 pc for an assumed distance of 1.25 kpc (see below). In this context, the observed anomalous proper motions can be regarded as an argument for the pertainance of all the associations to a single structure, placing them within a limited range of distances.

In view of these problems, it is difficult to adopt an average distance for the whole structure. Several lines of evidence, discussed by CTGJ93, seem to favour a distance in the range 1.0 - 1.6 kpc, and those authors adopt a value of 1.2 kpc in their study. They also notice that the distance to Cygnus OB2 can be made compatible with this value if a consistent calibration is used. This range is compatible with those derived by Garmany & Stencel 1992 for Cygnus OB1, OB3, and OB9. Published distances to the association in the eastern edge, Cygnus OB7, summarized by those same authors, tend to be smaller, about 800 pc. However, this is a sparse association for which distance determinations based on main sequence fitting may be severely biased by non members.

Although a solution to the distance uncertainty is beyond the scope of this paper, we have examined the problem using a kinematically selected sample, formed by the stars fulfilling

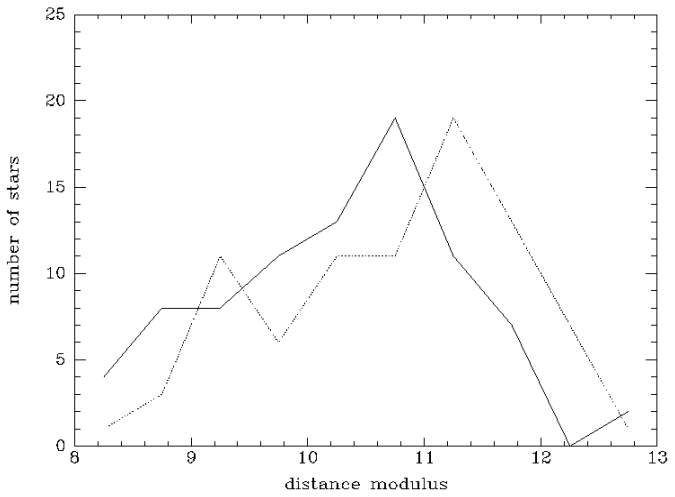

Fig. 4. Histograms of the distribution of distance moduli (DM) of "kinematic" members of the Cygnus expanding region, selected according to condition (3). The solid line corresponds to an adopted total-to- selective extinction ratio R_V = 4.0, and the dashed line to the standard value R_V = 3.1. In this latter case, the contribution to the peak at $DM \sim 9$ comes almost entirely from the lightly reddened stars in the eastern part of the region

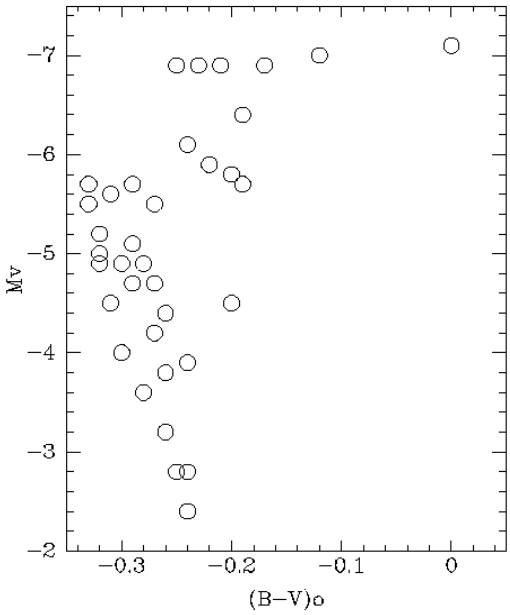

Fig. 5. HR diagram of the candidate members of the Cygnus expanding structure. Stars are plotted according to their spectral type, with absolute magnitude M_V and intrinsic color index $(B-V)_0$ from Schmidt-Kaler 1982.

the condition (3). For these stars, we used the spectral types and broad band photometric data (B and V magnitudes) from the *Hipparcos* Input Catalogue (see Sect. 2), and the absolute visual magnitude M_V and intrinsic color $(B-V)_0$ as a function of spectral type and luminosity class tabulated by Schmidt-Kaler 1982. We excluded from our sample stars with unknown or uncertain luminosity class. Distance moduli (DM) were then determined from

$$DM = V - M_V - R_V E(B-V) \quad (4)$$

where $E(B-V) = (B-V)-(B-V)_0$, and $R_V = A_V/E(B-V)$ is the total-to-selective extinction ratio. Using the standard value R_V = 3.1, we obtained a broad distribution of DM, represented by the dotted line in Fig. 4.

An important source of uncertainty in Eq. (4) comes from the adopted value of R_V, especially for the heavily reddened stars in the western part of the Superbubble. It is well known that R_V tends to be higher in star forming regions (Mathis 1990). We thus repeated the DM estimate using the value R_V = 4 found by Terranegra et al. 1994 for Cygnus, obtaining the histogram represented by the solid line in Fig. 4. This latter value reduces the distance scatter and the differences between the eastern and western side of the Superbubble, and is in better agreement with the proposed scenario of a single structure. The average value of the distance modulus in this case, which we will adopt henceforth, is DM = 10.5. Using other magnitude-spectral type calibrations for massive stars (Humphreys & McElroy 1984, Corbally & Garrison 1984) can produce large variations in the distances to some individual stars, but the peak of Fig. 4 is shifted by no more than $\sim$ 150 pc in either direction.

We have selected the sample of candidate members of the Cygnus expanding structure presented in Table 2. This list is composed by the stars fulfilling condition (3), with known spectral type and luminosity class, and having $9 < DM < 11.5$. The HR diagram of the stars in Table 2 is shown in Fig. 5. The main sequence turnoff near $M_V = -5.7$ indicates a very young age: comparing to the cluster HR diagrams of Meynet et al. 1993, and theoretical isochrones of Maeder & Meynet 1991, we estimate an age of $(5-10)\cdot 10^6$ yr.

4.2. The Canis Major region

The stellar population of the Canis Major OB1 - R1 complex has been studied in detail by Clariá 1974 and Eggen 1978. Its distance is about 1150 pc, and the age of the OB association is about $1.5\cdot 10^6$ yr (Clariá 1974). The age of the stellar population of the R association is estimated to be 10^5 - 10^6 yr (Herbst et al. 1978). Among the clusters present in the area, Clariá 1974 found that only NGC 2353 was probably related to Canis Major OB1 based on its derived age. However, the detailed study by Fitzgerald et al. 1990 seems to rule out this possibility, given their derived age of $7.6\cdot 10^7$ yr for NGC 2353.

Again, we found distance moduli for the stars of Canis Major using spectral type - absolute magnitude - color calibrations, with the data in the *Hipparcos* Input Catalogue. It can be seen in Fig. 6 that the bulk of the stars are distributed in the range $9.5 < DM < 11.5$. The choice of R_V is not critical now, given the generally low reddening in the region; we have used R_V = 3.1. The second peak in the distribution of DM seen in Fig. 6 possibly corresponds to a distant background population

Table 3. Candidate members of the Canis Major expanding structure

HIC	$l(^0)$	$b(^0)$	$\mu_l \cos b$ (mas yr^{-1})	μ_b (mas yr^{-1})	V	$(B-V)$	spectral type
34097	228.14	-4.09	-3.56	-2.53	8.39	0.00	B2/B3III
34133	224.80	-2.26	-3.80	-1.19	7.22	0.00	B0V
34234	224.17	-1.60	-2.29	-1.80	6.50	-0.06	B0.5IVn
34325	224.88	-1.67	-5.16	-2.26	7.62	-0.01	B1V
34395	225.51	-1.73	-4.30	-4.91	8.77	0.03	B2V
34443	225.51	-1.60	-3.32	-3.80	7.72	0.00	B2IIIn
34454	226.45	-2.04	-1.56	-3.03	7.20	-0.02	B2IV
34536	224.28	-0.69	-3.56	1.13	6.23	-0.02	O6
34561	229.54	-3.36	-0.07	-1.40	6.00	0.04	B1Ib/II
34616	229.11	-2.98	-1.08	-1.96	7.33	-0.08	B1III
34839	224.21	0.25	-2.66	4.30	8.47	0.09	B2Ve
34852	229.24	-2.34	-1.97	-2.14	7.85	-0.05	B2Vne...
35263	228.40	-0.70	-2.03	-1.11	7.74	-0.01	B3III
35707	224.53	2.71	-8.14	14.98	6.42	-0.19	O9V

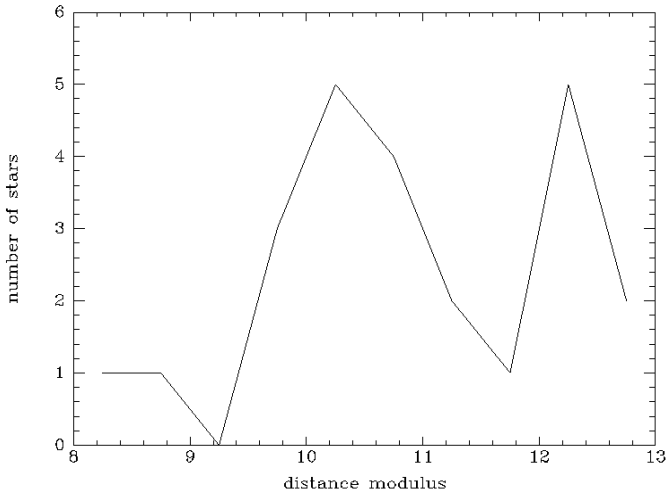

Fig. 6. Histogram of the distribution of distance moduli (DM) of "kinematic" members of the Canis Major expanding region, selected according to condition (3). A standard total-to-selective extinction ratio R_V = 3.1 was adopted.

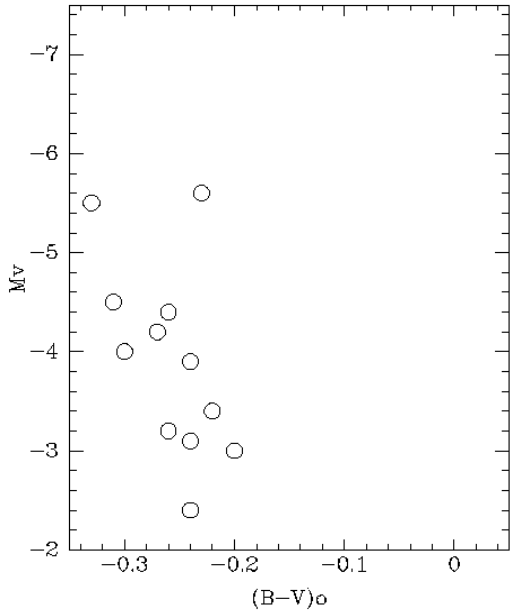

Fig. 7. HR diagram of the candidate members of the Canis Major OB1 / R1 iexpanding structure. Stars are plotted according to their spectral type, with absolute magnitude M_V and intrinsic color index $(B-V)_0$ from Schmidt- Kaler 1982.

already discussed by Fitzgerald et al. 1990. The main peak at $\sim$ 10.2 corresponds to a distance close to the 1150 pc determined by Clariá 1974, which we adopt here. The HR diagram of the candidate members is shown in Fig. 7. The scarcity of members makes it difficult to estimate the age, but we can consider it consistent with the estimates discussed above.

The gaseous component associated to Canis Major OB1 - R1 has been the object of numerous studies. The gas column density is traced by the IRAS far infrared emission, whose contours are overlaid on Fig. 3. The concentration around l = 224^0, b = -2.5^0 contains the association of reflection nebulae Canis Major R1 and several HII regions (S292, S293, S295, S296, S297; Gaylard & Kemball 1984). The R association lies mostly outside the arc-shaped pattern defined by the O and B stars. Herbst & Assousa 1977 summarized the available observations at the time, including the discovery of an expanding HI ring, and found support for the hypothesis that star formation in the region was triggered recently by an explosive event. Further evidence is supplied by observations of ionized (Reynolds & Ogden 1978) and molecular gas (Machnik et al 1980), confirming the existence of expanding motions. The onset of Parker instabilities triggering star formation in the region has been discussed by Baierlein et al. 1981 and Baierlein 1983. The magnetic field pattern predicted by this model was was indeed detected by Vrba et al. 1987.

The existence of a runaway star with a large radial velocity in the association, HIC 34536 (=HD 54662) has been known since

long ago (Neubauer 1943). Herbst & Assousa 1977 suggested that HIC 34536 could be the companion of the massive star which triggered star formation in the Canis Major complex, in the spirit of the hypothesis of Blaauw 1964 on the origin of runaway stars. The *Hipparcos* proper motions show that the residual space velocity vector is nearly parallel to the line of sight. This, together with the location of the star near the rim of bright nebulosity, rather than near its center of curvature, makes this interpretation less likely. However, the *Hipparcos* data reveal another runaway star, HIC 35707 (=HD 57682), whose residual velocity projected in the plane of the sky at the distance of the association is about 90 km s^{-1}. To our knowledge, its runaway nature has not been recognized before, having been classified as non-runaway by Gies 1987. Further indirect evidence for its runaway character comes from the extended emission around the star seen in IRAS maps at wavelengths of 25 μm and longer, possibly associated to a bow shock, as seen around other runaway stars (Noriega-Crespo et al. 1997). Its estimated distance (Berghöfer et al. 1996) is 1250 pc, well compatible with the distance of the association, and its radial velocity of 24 km s^{-1} (Buscombe & Kennedy 1968) differs by less than 10 km s^{-1} from that expected from galactic rotation and solar motion. Its velocity vector is thus roughly perpendicular to the line of sight and, when traced back in time, it passes very close to the estimated center of expansion at a time of $\simeq 10^6$ yr before the present. We therefore conclude that HIC 35707 is a much better candidate to be the companion of the possible massive star which started star formation in Canis Major OB1 - R1.

5. The origin of the expanding structures

5.1. Triggered star formation in Cygnus

The new data available allow us to reassess the proposed mechanisms for star formation in Cygnus and Canis Major. In the case of Cygnus, the presence of Cygnus OB2 near the center of expansion given in Table 1 suggests a time-sustained injection of energy as the powering source of the expansion of the Cygnus Superbubble. Neglecting losses by radiation inside a wind blown bubble, a constant energy injection rate produces a growth of its radius R with time of the form

$$R = 0.76(\frac{E_w\ t^3}{\rho_0})^{1/5} \tag{5}$$

where $E_w = \frac{1}{2}\dot{M}_w v_\infty^2$ is the mechanical power of the stellar wind, $\dot{M}_w$ being the stellar mass loss rate and v_∞ the wind terminal velocity (Weaver et al. 1977). The density of the ambient medium is ρ_0. In the case of a stellar aggregate, rather than a single star, E_w is the sum of the wind mechanical power of the member stars, plus the average energy input of each supernova explosion divided by the average interval between supernovae (Mac Low & McCray 1988). Eq. (5) is valid when the age of the bubble exceeds the cooling time of the collisionally heated gas accumulated by the expansion. This happens very early in the life of the bubble (Weaver et al. 1977), and for the ages of interest here we can consider that the validity of (5) extends practically back to $t = 0$. The bubble is thus surrounded by a dense shell whose surface density is approximately equal to the mass initially contained in the volume of the bubble, divided by its surface. Although thermal conduction evaporates material from the shell to the hot bubble interior, the evaporation rate is much smaller than the rate of accumulation of ambient gas onto the shell (Shull & Saken 1995).

Eventually, the dense shell surrounding the bubble can become unstable against its own gravity. Stability studies of the expanding shell have been presented by Vishniac 1983, McCray & Kafatos 1987, Elmegreen 1992, 1994, and CT94. Assuming that stars formed in this way move ballistically after the onset of the instability, when the bubble has an age t_0, the expansion law (5) predicts a simple pattern of proper motions as a function of the distance to the center of expansion projected in the plane of the sky: taking the time derivative of (5), the expansion velocity V at time t is

$$V = 0.46(\frac{E_w}{\rho_0 t^2})^{1/5} \tag{6}$$

Taking t as the present age of the bubble, the projected distance R_p to the center of expansion of a star formed at t_0 and observed now should be

$$R_p = \sin i[R(t_0) + V(t_0)(t - t_0)] \tag{7}$$

where i is the angle between the direction of expansion and the line of sight. The projected velocity v_P is

$$V_p = \sin i V(t_0) \tag{8}$$

Combining Eqs. (5)-(8), and dividing the resulting expression by the distance to the Sun to leave it in terms of the angular distance to the center of expansion λ and the modulus of the residual proper motion μ,

$$\lambda = (\frac{2}{3}t_0 + t)\mu \tag{9}$$

The constraint $0 < t_0 < t$ implies that λ and μ are proportional by a factor that can vary between t and $\frac{5}{3}t$. A plot of μ vs. λ for the candidate members listed in Table 2 is shown in Fig. 8.

If stars were formed by gravitational instability in the expanding shell, they should be found beyond its present limits, since they have been moving with the initial velocity while the shell was deccelerating by accumulation of ambient gas. The distance R_* to the center of expansion of stars formed at t_0 to the center of the shell should exceed the present shell radius R_S by a factor

$$\frac{R_*}{R_b} = (\frac{t_0}{t})^{3/5}(\frac{2}{5} + \frac{3}{5}\frac{t}{t_0}) \tag{10}$$

It can be seen indeed in Fig. 2 that stars with expanding motion are found outside the approximate boundaries of the Cygnus Superbubble.

The presently measured stellar velocities V_0 can be used to estimate the energetic output of the OB association powering

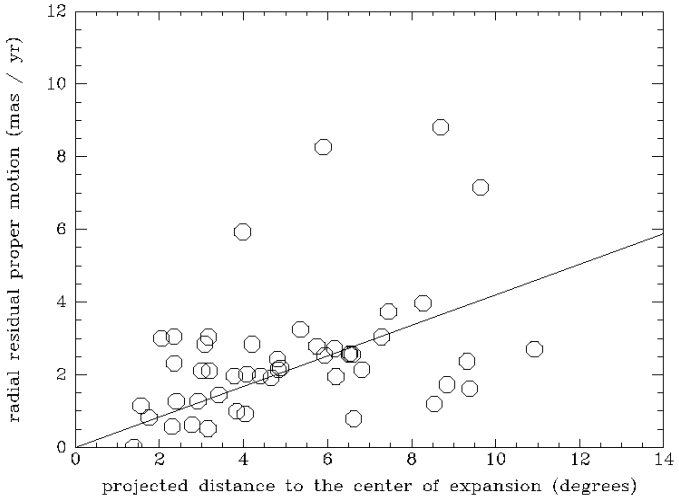

Fig. 8. Component of residual proper motion along the direction of expansion, plotted against the angular distance of candidate members of the Cygnus expanding structure to the center of expansion (given in Table 1). The best fit to the relationship given by Eq. (9) is indicated by the solid line, calculated taking into account only the non-runaway members.

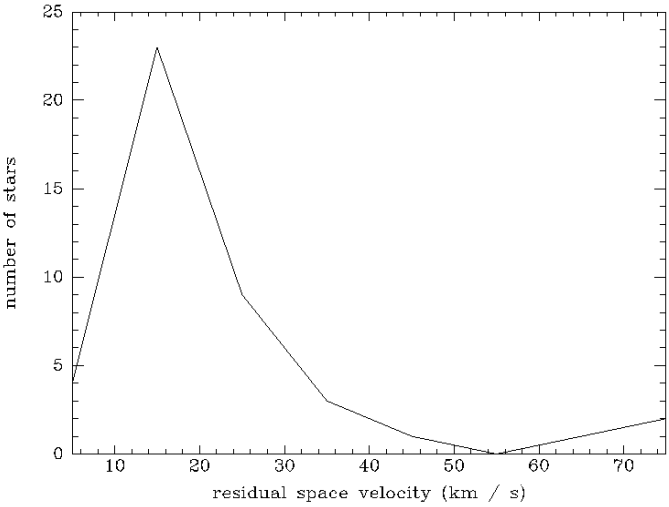

Fig. 9. Histogram of space velocities of the stars of our sample having measured radial velocities. The typical uncertainty in the radial velocity is $\sim$ 15 km s^{-1}, about three times larger than in tangential velocity, and this can cause some smear in the bins. However, the gap between the runaways and the rest of the stars is clearly seen.

the expansion. CT94 found a simple expression relating both quantities:[2]

$$E_w = 80.8 \frac{c}{G} V_0^4 \tag{11}$$

where c is the effective sound speed in the shell, and G is the gravitational constant. The shell becomes unstable at an age

$$t_0 = 1.29 (\frac{c}{G})^{5/8} L^{-1/8} \rho^{-1/2} \tag{12}$$

Adopting c = 1 km s^{-1} and the largest velocities plotted in Fig. 8, i.e, $V_0 \simeq 65$ km s^{-1}, one obtains

$$E_w \sim 2.1 \cdot 10^{41} \text{ erg s}^{-1}.$$

This is by far much more than stellar activity alone can provide: the power required is equivalent to one supernova every 150 years! Nevertheless, the energetic requirements become much more relaxed if the fastest moving stars are actually runaways, whose large velocities have a different origin. The production of runaway stars in a rich and dense association like Cygnus OB2 must have been abundant in either of the usually invoked hypothesis on their origin (Gies 1987): the supernova explosion of a massive companion in a close binary system (see also Sect. 4.2), or the dynamical ejection of massive stars in dense stellar environments.

To further confirm the runaway nature of the fastest-moving stars in the region, we complemented the *Hipparcos* proper motions with radial velocities from the literature, mostly from Evans 1967. Our results show that, out of 7 stars with residual proper motions $\mu_{res} > 4$ mas yr^{-1}, 5 have radial velocities deviating by more than 20 km s^{-1} from that expected from galactic rotation and proper motion alone; another one, HIC 101186 (=HD 195592), is a O9.5Ia star with a detected bow shock ahead of it (Noriega-Crespo et al. 1997), characteristic of runaway stars; and the seventh one, HIC 101729, does not have measurements of the radial velocity in the literature. To support the independent origin of the fastest moving stars, we plot in Fig. 9 the histogram of residual space velocities for all the stars in Table 2 with measured radial velocities. A clear gap exists between 45 and 60 km s^{-1}, separating the bulk of stars from the likely runaways.

The 4th power in the velocity in Eq. (11) dramatically decreases the energetic requirements on Cygnus OB2 when the runaways are excluded. Given the much lower precission of the radial velocities as compared to the *Hipparcos* tangential velocities at the distance of Cygnus, the rather high upper limit of 45 km s^{-1} for non-runaway stars probably results from errors in radial velocity measurements. Therefore, we use only proper motions in our estimate of V_0, assuming that the stars having the largest proper motion move in the plane of the sky and were formed at the time t_0 when the shell became unstable. The largest non-runaway expansion velocities appearing in Fig. 8 imply $V_0 \simeq 25$ km s^{-1}, and thus

$$E_w = 4.7 \cdot 10^{39} \text{ erg s}^{-1}.$$

As already discussed by CT94, there are considerable uncertainties in establishing a comparison between the estimated E_w and the observational characteristics of Cygnus OB2. The uncertainties arise from the large simplifications introduce in

[2] The numerical factors in Eqs. (11) and (12) are greater than those in Eqs. (30) and (18) of CT94. The difference arises from a factor 2 missing in the second term of the left- hand side in Eq. (10) of that paper. We thank Dr. B.G. Elmegreen for having pointed out that mistake to us.

the linear perturbation analysis leading to Eq. (11), the adopted value of c, and the difficulties in estimating the energy output of Cygnus OB2 from existing observations. We have carried out a rough estimate of this output using mass-luminosity and mass-temperature relationships for massive stars in the main sequence (Lang 1991), together with stellar wind parameters given by Leitherer et al. 1992 In this way, we obtain for a main sequence star of mass M and solar metallicity:

$$E_w^*(\mathrm{erg\ s^{-1}}) = 2.2 \cdot 10^{31} M(\mathrm{M_\odot})^{3.0} \quad (13)$$

where the asterisk in E_w^* indicates an individual star. We then estimate the total energy injected by stellar winds by integrating Eq. (13) over the whole mass range, weighing it with the initial mass function. We use the IMF found by Massey et al. 1995 for Cygnus OB2, transformed to linear (rather than logarithmic, as given by those authors) mass intervals:

$$N(M)\, dM = AM^{-1.9}\, dM \quad (14)$$

Also following Massey et al. 1995, we assume a cutoff mass of 120 $\mathrm{M_\odot}$. The integrated mechanical power is then

$$E_w = 2.1 \cdot 10^{35} A \quad (15)$$

The scale factor A is calculated from the number of massive stars observed in the association. If $N(> 10\mathrm{M_\odot})$ is the number of stars with masses over 10 $\mathrm{M_\odot}$, Eq. (13) becomes:

$$E_w = 1.7 \cdot 10^{36} N(> 10\mathrm{M_\odot}) \quad (16)$$

The energetic considerations based on the gravitational instability scenario thus require about 2800 stars, about 30 times greater than the number of stars more massive than 10 $\mathrm{M_\odot}$ counted by Massey et al. 1995. However, E_w as given by Eq. (16) is rather a lower limit for several reasons:

a) As pointed out by those authors, their survey of Cygnus OB2 is estimated to be incomplete for masses below ~ 15 $\mathrm{M_\odot}$.

b) Many members of Cygnus OB2 are heavily obscured and even massive stars may have been undetected (Parthasarathy & Jain 1995).

c) The existence of evolved massive stars sugests that the association had more very massive stars in the past, which have exploded as supernovae. The mentioned existence of runaway stars moving away from Cygnus OB2 may be interpreted as an evidence for past supernovae in the association. Such evolution of the massive end of the stellar mass distribution implies that the present-day mass function, whose slope is derived by Massey et al. 1995, is steeper than the initial mass function.

d) Undetected binarity with components of similar mass, common among OB stars, is not taken into account in the derivation of the mass function.

e) The derivation of the mass function is sensitive to the adopted evolutionary tracks; compare for example Massey & Thompson 1991 with Massey et al. 1995.

All those factors, with the only possible exception of the fifth one, increase the estimate of E_w, and may easily bring it to less than one order of magnitude from the estimate derived from Eq. (11). Given the crude approximations involved in all the steps of the comparison, the agreement can be considered as acceptable.

The observation of non-runaway stars moving away from the center of expansion and lying at distances greater than the major axis of the Superbubble permits and approximate dating of the structure and of the onset of the gravitational instability. We take the slope of the fit to the non-runaway stars in Fig. 8 as $(\frac{2}{3}t_0 + t)$, use Eq. (10), and assume that t_0 is the time when the shell first becomes unstable. Estimating R_*/R_b to be ~ 1.25 from Figs. 2 and 8, Eq. (10) gives $t_0/t \simeq 0.25$; the slope of the $\lambda - \mu$ relationship is $(\frac{2}{3}t_0 + t) \simeq 8.5 \cdot 10^6$ yr. Formation of stellar systems in the shell is thus estimated to have started $t - t_0 \simeq 5.5 \cdot 10^6$ years ago.

On the other hand, we estimate from Eq. (12) that the ambient density of the medium where the bubble expands is $n_H \simeq 40$ g cm^{-3}. This density is between that of the diffuse interstellar medium and that of giant molecular clouds where OB associations form (Blitz 1993). Given that the present size of the structure exceeds that of the largest molecular clouds, it is likely that the Superbubble initially expanded in a denser medium typical of the conditions in molecular clouds, and then proceeded in a lower density medium after reaching the boundaries of the cloud. This complicates the evolution of the bubble and renders Eq. (10) inapplicable, but a consequence of the expansion in a more dense medium would be that the gravitational instability would appear at earlier times and the associations would be older than the estimate given in the previous paragraph. We can thus roughly date them between 5.5 and $8.5 \cdot 10^6$ yr, in agreement with the appearance of their HR diagram. On the other hand, an age of $8.5 \cdot 10^6$ yr for Cygnus OB2 is consistent with the lower limit of $3 \cdot 10^6$ yr found by Torres-Dodgen et al. 1991, and is somewhat higher than the interval of $(1 - 4) \cdot 10^6$ yr quoted by Massey et al. 1995, although the uncertainties are considerable. An independent, simple lower limit to the age of Cygnus OB2 comes from the identified runaway stars: their kinematic ages range from $2.4 \cdot 10^6$ yr for HIC 101186 to $4.9 \cdot 10^6$ yr for HIC 104361 (a higher value, $7.1 \cdot 10^6$ yr, is given by HIC 100409; but the tangential velocity is small, making the estimate uncertain by more than 30 %). Taking into account that, if the runaways come from the disruption of a binary system, the primary existed for some time before exploding as a supernova, we find that these ages are in agreement with the timescale derived from gravitational instability considerations.

5.2. Triggered star formation in Canis Major

The expanding motions detected in Canis Major differ from those of Cygnus in several significant aspects. First, the absence of a cluster or association at the center of the expansion tends to favour a single explosive event as the trigger of star formation. Secondly, the stars lie between the kinematic center of expansion and the densest concentration of molecular gas, where star formation is taking place at present. This is unlike the case of Cygnus, where the stellar expanding motions extent beyond the limits of the Superbubble and the Hα filaments

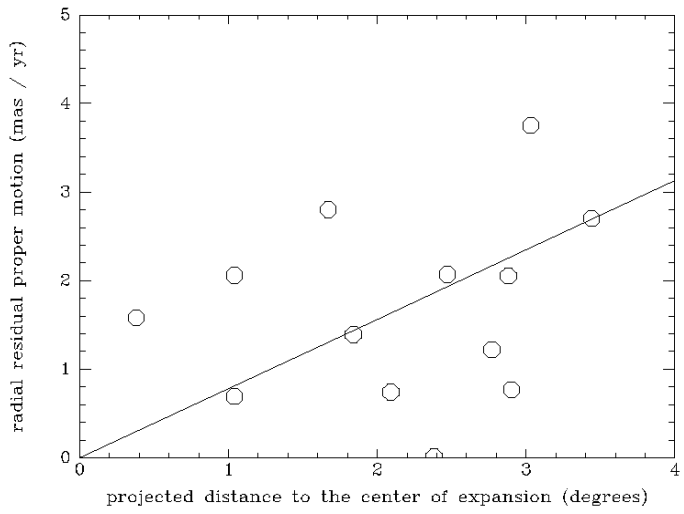

Fig. 10. Angular distance of candidate members of the Canis Major structure to the center of expansion (given in Table 1), plotted against the component of residual proper motion along the direction of expansion. The probable runaway star HIC 35707, with a residual proper motion μ = 17.0 mas yr^{-1}, has been left out of the plot

roughly delineating it. A third difference is the magnitude of the motions in Cygnus, almost twice as large as those in Canis Major. The diagram of proper motions as a function of distance to the center of expansion is presented in Fig. 10, from where a maximum expansion velocity of $\simeq$ 15 km s^{-1} is estimated. This value is larger than, but comparable to, the velocity dispersion measured in nearby asssociations. If Canis Major OB1 had been formed as a compact, unbound group, the internal velocity dispersion would naturally produce a radially expanding pattern as the association disperses. Nevertheless, in that case the expansion should be isotropic, which clearly is not the case for Canis Major OB1.

Reviews of the theory of supernova remnants can be found in Woltjer 1972, Dyson & Williams 1980, Reynolds 1988, Shu 1992, and Bisnoviatyi-Kogan & Silich 1995. Several stages can be distinguished in the expansion of the bubble produced by a supernova: the initial free expansion of the supernova ejecta is followed by the Sedov phase, in which the ambient interstellar gas is shock-heated to very high temperatures and incorporated to the interior of the bubble. As the expansion deccelerates, the cooling time of the shocked interstellar gas decreases below the expansion rate of the bubble, and radiative losses begin to be important in the interior. A dense shell forms around the bubble, whose expansion is due to momentum conservation. At late ages, the radius R grows as

$$R = (\frac{10 E_{SN} t}{3\pi\rho_0 v_{trans}})^{1/4} \quad (17)$$

where E_{SN} is the kinetic energy released by the supernova, ρ_0 is the ambient density, and v_{trans} is the velocity of the shock propagating into the ambient medium at the time of transition from the Sedov to the momentum-conserving phase; calculations indicate that $v_{trans} \simeq 200$ km s^{-1} under a broad range of conditions (Woltjer 1972). Introducing this expansion law in the equations used by CT94 to derive their criterion of gravitational instability in an expanding shell, we obtain that, at the onset of the gravitational instability, the expansion velocity V_{ins} should be

$$V_{ins} = 0.5022(\frac{G^3 \rho_0 E_{SN}^2}{c^3 v_{trans}^2})^{1/5} \quad (18)$$

Using as typical parameters $E_{SN} = 10^{51}$ erg, $\rho_0 = 2.3 \cdot 10^{-24}$ g cm^{-3}, and c = 1 km s^{-1}, we obtain $V_{ins} \simeq 1.4$ km s^{-1}, well below the effective sound speed in the interstellar medium. Given the $1/5$ exponent in Eq. (18), this estimate is not very sensitive to changes in the input parameters, and clearly shows that gravitational instability in a supernova remnant cannot be the mechanism having triggered the formation of Canis Major OB1.

A simpler and more viable alternative is the acceleration and compression of a hemispherical shell of moderate density by a supernova explosion. Such a shell can be expected to be produced naturally by the photoionization and stellar winds from the supernova precursor along its evolution, if it lies near the boundary of the molecular cloud where it was formed. The results are *champagne* flows which disrupt a part of the cloud before the supernova explosion (Tenorio-Tagle 1982, Comerón 1997). The evolution of a supernova exploding in the cavity around the precursor produced by a *champagne* flow was simulated by Yorke et al. 1989; the acceleration of the remnants of the molecular cloud was not considered in that study, however, as the cloud was taken to have an indefinite extent in the direction opposite to the *champagne* flow.

To consider the viability of the proposed hypothesis, let us consider a supernova ejecting a mass M_{ej} at a velocity v_{ej}. The momentum of the ejecta is transmitted to the hemispherical shell centered on the star with mass M_s, which is thus accelerated to a velocity v_s. Assuming as typical parameters M_{ej} = 1 M$_\odot$, v_{ej} = 10,000 km s^{-1} (thus giving $E_{SN} = 10^{51}$ erg), and taking v_s = 15 km s^{-1} as the expansion velocity of the members of Canis Major OB1, the mass of the shell that can be accelerated in this way is

$$M_s \sim M_{ej} \frac{v_{ej}}{2 v_s} \quad (19)$$

This gives $M_s \simeq 300$ M$_\odot$. The actual value of M_s may be expected to be greater than this, given that the shell should be already accelerated before the supernova explosion by the stellar wind and by the expansion of the HII region around the precursor, whose momentum injection can be comparable to that of the supernova (Dyson & Williams 1980); $M_s \simeq 1,000$ M$_\odot$ may be a more realistic value. To make the gravitational collapse of the shell possible, its radius r must be at least of order of a critical wavelength $\lambda \sim (c^2/G\sigma)$ (Larson 1985), with the surface density $\sigma = (M_s/2\pi r^2)$. Taking into account the large uncertainties involved in our estimate of all the involved parameters, we find that a compressed shell with mass 1,000 M$_\odot$, density 10^4 cm^{-3}, and radius and thickness of order $\sim$ 1 pc may provide the initial conditions required. On the other hand,

the momentum injected by the supernova in other directions where the ambient gas column density is lower would accelerate it to higher velocities. This could explain the fact that the region of current star formation, Canis Major R1, lies beyond the OB association as seen from the center of expansion, as well as the higher expansion velocity of the HI shell found by Herbst & Assousa 1977 with respect to the expansion velocity of the OB association.

We should emphasize the tentative nature of the explanation proposed here. As already remarked by Herbst & Assousa 1977, it is difficult to find at the present direct evidence supporting the supernova scenario. If the event took place over one million years ago, none of the typical observational signatures of younger supernova regions in the different spectral regions should be detectable anymore. The hypothesis proposed here to account for the origin of the motions of the stars in Canis Major OB1 should thus be taken as an explanation consistent with a number of facts, such as the spatial arrangement and age of the different structures, the kinematical pattern, the runaway HIC 35707, and the compatibility of a supernova explosion with the energetic requirements implied by the observed motions.

6. Summary

We have studied the patterns of expanding motions measured by the *Hipparcos* satellite in two stellar complexes, one in the area occupied by the Cygnus Superbubble and the other coincident with the Canis Major OB1 - R1 region. Tangential velocities in both regions exceed the values that would be expected from the internal velocity dispersion in OB associations. The pattern of the expansion and the spatial arrangement of the stellar population can be linked to observations of the gaseous component carried out in other wavelengths. In this way, the emerging picture is suggestive of very energetic events both having triggered the formation of massive stars and being the cause of the expanding motions.

In the case of Cygnus, it is found that the association Cygnus OB2 lying near the center of the Superbubble may have triggered star formation in a shell caused by the energetic output of its massive stars. The collapse of parts of this shell under its own gravity would then have given rise to the stars in the OB associations located in the periphery of the Superbubble (Cygnus OB1, OB3, OB7, and OB9), whose present-day motions would thus reflect the expansion of the shell at the time of becoming unstable. The energetic requirements of this scenario have been discussed and compared to published observations of Cygnus OB2; consistency is found within the large uncertainties involved, which arise both from the observations and from modelling oversimplifications. It seems clear that the proposed mechanism cannot work if the fastest-moving stars in the region were formed by the same process. However, a likely explanation is that stars with velocities exceeding 40 km s^{-1} are actually runaways from Cygnus OB2 whose origin is unrelated to the shell. There is indeed a gap in the histogram of space velocities separating these runaway candidates from the overall expanding population.

As for the Canis Major region, a supernova explosion has been proposed in the past as the mechanism responsible for star formation in Canis Major R1, an association of reflection nebulae and HII regions in the southwestern corner of the OB association. Further support for this hypothesis is found in the existence of a new runaway star revealed by its large proper motion directed away from the center of expansion. The newly found motions of the O and B stars are suggestive of them having their origin also in the same event. It is found that the hypothesis of a gravitational instability in a supernova shell, similar to that proposed for Cygnus, cannot account for the observed velocities. Instead, it seems more plausible that the stars were formed out of the remnants of the molecular cloud where the supernova precursor was formed in the first place, probably having produced a *champagne* flow episode during its early evolution. The surviving portion of the cloud, with an estimated mass of $\sim 1,000\,M_{\odot}$, would have been accelerated by both the expansion of the HII region and the stellar wind produced by the supernova precursor, as well as by the supernova explosion itself.

Acknowledgements. Comments of an anonymous referee leading to improvements in this paper are appreciated. JT acknowledges support of the CICYT under contract ESP95-0180. The work of JT and AEG is also supported by the program *Acciones integradas hispano-francesas*. This work made use of the SIMBAD database maintained at the Centre de Données Stellaires, Strasbourg.

References

Abbott, D.C., Bieging, J.H., Churchwell, E., 1981, ApJ, 250, 645.
Alvarez, H., May, J., Bronfman, L., 1990, ApJ, 348, 495.
Baierlein, R., 1983, MNRAS, 205, 669.
Baierlein, R., Schwing, E., Herbst, W., 1981, Icarus, 48, 49.
Berghöffer, T.W., Schmitt, J.H.M.M., Cassinelli, J.P., 1996, A&AS, 118, 481.
Bisnoviatyi-Kogan, G.S., Silich, S.A., 1995. Rev. Mod. Phys. 67, 661.
Blaauw, A., 1964, ARA&A, 2, 213.
Bochkarev, N.G., Sitnik, T.G., 1985, Ap&SS, 108, 237.
Brand, P.W., Zealey, W.J., 1975, A&A, 38, 363.
Buscombe, W., Kennedy, P.M., MNRAS, 139, 341.
Cash, W., Charles, P., Bowyer, S., Walter F., Garmire, G., Riegler, G., 1980, ApJ, 238, L71.
Clariá, J.J., 1974, A&A, 37, 229.
Clemens, D., 1985, ApJ, 295, 422.
Comerón, F., 1997, A&A, in press.
Comerón, F., Torra, J., 1992, A&A, 261, 94.
Comerón, F., Torra, J., 1994a, ApJ, 423, 652 (CT94).
Comerón, F., Torra, J., 1994b, A&A, 281, 35.
Comerón, F., Torra, J., Jordi, C., Gómez, A.E., 1993, A&AS, 101, 37 (CTGJ93).
Comerón, F., Torra, J., Gómez, A.E., 1994, A&A, 286, 789.
Comerón, F., Torra, J., Figueras, F., 1997, A&A, 325, 149.
Corbally, C.J., Garrison, R.F., 1984, in "The MK process", David Dunlap Obs.
Dewdney, P.E., Lozinskaya, T.A., 1994, AJ, 108, 2122.
Domgoergen, H., Bomans, D.J., De Boer, K.S., 1995, A&A, 296, 523.
Dyson, J.E., Williams, D.A., 1980, "The physics of the interstellar medium", Manchester Univ. Press.

Eggen, O.J., 1978, PASP, 90, 436.
Elmegreen, B.G., 1992, in "Star formation in stellar systems", eds. G. Tenorio-Tagle, M. Prieto, F. Sánchez, Cambridge Univ. Press.
Elmegreen, B.G., 1994, ApJ, 427, 384.
Elmegreen, B.G., Lada, C.J., 1977, ApJ, 214, 725.
Elmegreen, B.G., Kimura, T., Tosa, M., 1995, ApJ, 451, 675.
Elmegreen, D.M., 1985, in "The Milky Way Galaxy", D. Reidel.
Evans, D.S., 1967, IAU symp, 30, 57.
Fitzgerald, M.P., Harris, G.L., Reed, B.C., 1990, PASP, 102, 865.
Garmany, C.D., Stencel, R.E., 1992, A&AS, 94, 211.
Gaylard, M.J., Kemball, A.J., 1984, MNRAS, 211, 155.
de Geus, E.J., 1990, in "Properties of hot luminous stars", ASP Conf. Ser.
Gies, D.R., 1987, ApJS, 64, 545.
Grabelsky, D.A., Cohen, R.S., Bronfman, L., Thaddeus, P., 1988, ApJ, 331, 181.
Herbst, W., Assousa, G.E., 1977, ApJ, 217, 473.
Herbst, W., Racine, R., Warner, J.W., 1978, ApJ, 223, 471.
Humphreys, R.M., 1976, PASP, 88, 647.
Humphreys, R.M., 1978, ApJS, 38, 309.
Humphreys, R.M., McElroy, D.B., 1984, ApJ, 284, 565.
Lang, K.R., 1991, "Astrophysical data: planets and stars", Springer-Verlag.
Larson, R.B., 1985, MNRAS, 214, 379.
Leitherer, C., Robert, C., Drissen, L., 1992, ApJ, 401, 596.
Lin, C.C., Yuan, C., Roberts, W.W., 1978, A&A, 69, 181.
Lindblad, P.O., Grape, K., Sandqvist, Aa., Schober, J., 1973, A&A, 24, 309.
Luri, X., 1995, PhD Thesis, Universitat de Barcelona.
Mac Low, M.-M., McCray, R., 1988, ApJ, 324, 776.
Machnik, D.E., Hettrick, M.C., Kutner, M.L., Dickman, R.L., Tucker, K.D., 1980, ApJ, 242, 121.
Maeder, A., Meynet, G., 1991, A&AS, 89, 451.
Massey, P., Thompson, A.B., 1991, AJ, 101, 1408.
Massey, P., Johnson, K.E., DeGioia-Eastwood, K., 1995, ApJ, 454, 151.
Mathis, J.S., 1990, ARA&A, 28, 37.
McCray, R., Kafatos, M., 1987, ApJ, 317, 190.
Meynet, G., Mermilliod, J.-C., Maeder, A., 1993, A&AS, 98, 477.
Myers, P.C., 1987, in "Interstellar Processes", eds. D.J. Hollenbach & H.A. Thronson, D. Reidel.
Neubauer, F.J., 1943, ApJ, 97, 300.
Noriega-Crespo, A., Van Buren, D., Dgani, R., 1997, AJ, 113, 780.
Odenwald, S., 1989, ApJ, 405, 706.
Odenwald, S., Schwartz, P.R., 1993, ApJ, 405, 706.
Oey, M.S., Massey, P., 1994, ApJ, 425, 635.
Oey, M.S., Massey, P., 1995, ApJ, 452, 210.
Olano, C.A., Pöppel, W.G.L., 1987, A&A 179, 202.
Palous, J., 1991, Mem. SAI, 62, 969.
Palous, J., Tenorio-Tagle, G., Franco, J., 1994, MNRAS, 270, 75.
Palous, J., Franco, J., Tenorio-Tagle, G., 1990, A&A, 227, 175.
Parthasarathy J., Jain, S.K., 1995, A&AS, 111, 407.
Phillips, A.P., Welsh, B.Y., Pettini, M., 1984, MNRAS, 206, 55.
Piepenbrink, A., Wendker, H.J., 1988, A&A, 191, 313.
Pöppel, W.G.L., 1997, Fund. Cosm. Phys. 18, 1.
Reynolds, S.P., 1988, in "Galactic and extragalactic radioastronomy", Eds. G.L. Verschuur, K.I. Kellerman, Springer-Verlag.
Reynolds, R.J., Ogden, P.M., 1978, ApJ, 224, 94.
Roberts, W.W., 1969, ApJ, 158, 123.
Rosado, M., Laval, A., Le Coarer, E., Georgelin, Y.P., Amram, P., Marcelin, M., Goldes, G., Gach, J.L., 1996, A&A, 308, 588.
Ruprecht, J., Balazs, B., White, R.E., 1981, "Catalogue of Star Clusters and Associations, Supplement 1: Associations", Akademiai Kiado, Publ. House Hungarian Acad. Sciences.
Saken, J.M., Shull, J.M., Garmany, C.D., Nichols-Bohlin, J., Fesen, R., 1992, ApJ, 397, 537.
Scheffler, H., Elsässer, H., 1987, "Physics of the Galaxy and the interstellar medium", Springer-Verlag.
Schmidt-Kaler, T., 1975, Vistas in Astronomy, 19, 69.
Schmidt-Kaler, T., 1982, in Landolt-Börnstein, Vol. 2b, eds. J. Schaifers & H.H. Voigt, Springer-Verlag.
Shu, F.H. 1992, "The physics of astrophysics, Vol. II: Gas dynamics", Univ. Science Books.
Shu, F.H., Milione, V., Gebel, W., Yuan, c., Goldsmith, D.W., Roberts, W.W., 1972, ApJ, 173, 557.
Shull, J.M., Saken, J., 1995, ApJ, 444, 663.
St.-Louis, N., Smith, L.J., 1991, A&A, 252, 781.
Tenorio-Tagle, G., 1982, in Regions of recent star formation, eds. R. Roger, P. Dewdnay, D. Reidel.
Tenorio-Tagle, G., Palous, J., 1987, A&A, 237, 207.
Terranegra, L., Chavarría, C., Díaz, S., González-Patino, D., 1994, A&AS, 104, 557.
Torres-Dodgen, A.V., Tapia, M., Carroll, M., 1991, MNRAS, 249, 1.
Turon, C., et al., 1992, "The Hipparcos Input Catalogue", ESA SP-1136.
Vallenari, A., Bomans, D.J., De Boer, K.S., 1993, A&A, 268, 137.
Vishniac, E.T., 1983, ApJ, 274, 152.
Vogt, N., Moffat, A.F.J., 1975, A&A, 39, 477.
Vrba, F.J., Baierlein, R., Herbst, W., 1987, ApJ, 317, 207.
Weaver, R., McCray, R., Castor, J., Shapiro, P., Moore, R., 1977, ApJ, 218, 377.
Wendker, H.J., 1984, A&AS, 58, 291.
Wendker, H.J., Higgs, L.A., Landecker, T.L., 1991, A&A, 241, 551.
Whitworth, A.P., Bhattal, A.S., Chapman, S.J., Disney, M.J., Turner, J.A., 1994, MNRAS, 268, 291.
Will, J.-M., Bomans, D.J., Vallenari, A., Schmidt, J.H.K., De Boer, K.S., 1996, A&A, 315, 125.
Woltjer, L., 1972, ARA&A, 10, 129.
Yorke, H.W., Tenorio-Tagle, G., Bodenheimer, P., Różyczka, M., 1989, A&A, 216, 207.

This article was processed by the author using Springer-Verlag LaTeX A&A style file *L-AA* version 3.